Sl. No.	IIT Ropar List of Recent Publications with Abstract Coverage: June, 2022
1.	(MLE^{2}A^{2}U)-Net: Image Super-Resolution via Multi-Level Edge Embedding and Aggregated Attentive Upsampler Network N Mehta, S Murala – IEEE Transactions on Emerging Topics in Computational Intelligence, 2022 **Abstract:** Given a degraded low-resolution input image, super-resolution (SR) aims at restoring the lost textures and structures and generating high-resolution image content. Significant advances in image super-resolution have been made lately, dominated by convolutional neural networks (CNNs). The top performing CNN-based SR networks typically employ very deep models for embracing the benefits of generating spatially precise results, but at the cost of loss of long-term contextual information. Additionally, state-of-the-art (SOTA) methods generally lack in maintaining the balance between spatial details and contextual information, which is the basic requirement for exhibiting superior performance in SR task. For restoration application like SR, the overall network generally demands efficient preservation of low-frequency information and reconstruction of high-frequency details. Thus, our work presents a novel architecture with the holistic objective of maintaining spatially-precise representation by collecting contextual content and restoring multi-frequency information throughout the network. Our proposed model learns an enriched set of features, that besides combining contextual information from multiple scales simultaneously preserves the high-resolution spatial details. The core of our approach is a novel non-local and local attention (NLLA) block which focuses on (1) learning enriched features by collecting information from multiple scales, (2) simultaneously handling the different frequency information, and (3) effectively fusing the relevant low-frequency and high-frequency information by ignoring the redundant features. Additionally, for effectively mapping the low-resolution features to high-resolution, we propose a novel aggregated attentive up-sampler (AAU) block that attentively learns the weights to up-sample the refined low-resolution feature maps to high-resolution output. Extensive experiments on the benchmark SR datasets demonstrate that the proposed method achieves appealing performance, both qualitatively and quantitatively.
2.	A Comprehensive Review on the Synthesis Techniques of Porous Materials for Gas Separation and Catalysis V Sharma, A Agrawal, O Singh, R Goyal, B Sarkar, N Gopinathan, SP Gumfekar – The Canadian Journal of Chemical Engineering, 2022 **Abstract:** Intrinsic structural characteristics of porous materials have found significant applications in selective separation of gases and heterogeneous catalysis. While using porous materials for gas separation and catalysis, some of the challenging issues are the strength of catalytic sites, hydrothermal stability, crystalline order of solids, and selectivity. Researchers' ability to engineer the synthesis strategies rationally can help overcome technological challenges. In recent years, breakthroughs in porous materials are focused on developing different chemistries to control the pore architecture. This review focuses on recent advances made in synthesis strategies of porous materials and their impact on gas separation and catalysis applications. A significant part of this review is devoted to various synthesis methods, such as various types of templating methods, molecular layer deposition, sol-gel technique, and polymerization methods. Improvement in various catalytic reactions and gas separations due to different functionalization methods is also summarized. Lastly, we have discussed the applications of porous materials in the form of adsorbents and membranes in commercial processes. We hope that this review will serve as a quick reference for beginners who want to

	synthesize porous materials with control of pore structure.
3.	A locking-free formulation for three-dimensional isogeometric analysis DS Bombarde, M Agrawal, SS Gautam, A Nandy – Materials Today: Proceedings, 2022 **Abstract**: Non-uniform rational B-splines (NURBS)-based isogeometric analysis (IGA) suffers from locking while analyzing highly slender geometries or problems dominated by incompressibility or near incompressibility constraint. The authors have recently proposed a class of reliable and efficient NURBS-based hybrid elements to alleviate locking in two-dimensional linear elasticity regime. Nevertheless, in several practical situations, the problem often necessitates the three-dimensional elements to analyze an accurate behavior of the domain. In the present work, novel stress-based elements are introduced to eliminate the adverse effects of locking in three-dimensional linear elastic NURBS-based IGA. The comprehensive assessment of several benchmark numerical examples shows the method's capabilities.
4.	A metal-free $BF_3{\cdot}OEt_2$ mediated chemoselective protocol for the synthesis of propargylic cyclic imines PR Singh, B Gopal, M Kumar, A Goswami – Organic and Biomolecular Chemistry, 2022 **Abstract:** A chemoselective and metal/additive-free protocol for the synthesis of propargylic cyclic imine derivatives via (3 + 2)-cycloaddition of donor-acceptor cyclopropanes and alkynylnitriles in the presence of $BF_3{\cdot}OEt_2$ has been established. The newly developed methodology provided access to a variety of propargylic cyclic imines in good to excellent yields. In addition, the synthesis of propargylic amines and the corresponding very stable enol derivatives from the title compound is also explored. 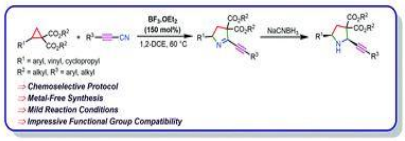
5.	A Multi-Coil Array Transceiver Antenna Design for Touchless Hygienic Artificial Human Interfacing VK Srivastava, A Bharadwaj, A Sharma – IEEE Transactions on Antennas and Propagation, 2022 **Abstract:** This paper presents an optimized multi-coil array transceiver antenna design to localize the position of a human hand for a touchless artificial human interface. The functioning of the system is evolved from combined principles of a 2-coil and 3-coil magnetic resonance coupling based wireless power transfer techniques. The proposed system comprises of a transceiver antenna platform made of spatially distributed multi-coil arrays as transmitter and receiver antennas, and a resonator coil. The resonator coil attached to the fingertip of the user is localized by comparing the voltage gains of the receiver antenna array working as sensors with the decision thresholds. Therefore, the coil arrays of the transceiver platform and the resonator coil are jointly optimized to enhance the localization accuracy by maximizing the separation of receiver antenna readings from the decision thresholds. The fabricated prototype of the optimized antenna system is measured, and performance is analyzed for various movements of the user fingertip. The result reveal the decision threshold limits of the design for localization and prove that the proposed transceiver antenna system is able to track the human hand movement successfully. Unlike other vision and sensor-based interfacing, the proposed transceiver antenna system provides a cost-effective, user-friendly, and hygienic solution.
6.	A Survey on Efficient Interconnects for Neuromorphic Systems S Kumar, S Das, G Badone, A Kumar – Soft Computing: Theories and Applications, 2022 **Abstract:** Neuromorphic computing is a trending area in computer architecture which deals with

	the simulation of the brain on hardware. Machine learning problems are very complex to solve by a simple computer that works based on Von Neumann architecture, so we need to find architectures that are inspired by the brain and efficient for machine learning, artificial intelligence, and more complex applications. Neuromorphic computing deals with how the brain works; another thing is to find the material for simulating the brain on hardware and efficient algorithm for neuromorphic architecture. Simulating the working of neurons on hardware is very challenging because of the structure of neurons and communication mechanisms. In this paper, we have discussed the challenges in designing the communication mechanism for such neuromorphic computing when implemented in hardware. Each node in such hardware needs to multicast a message to many other nodes. The existing on-chip interconnects architectures are not enough to support such communication. We are presenting a survey on neuromorphic computing algorithms and architecture that have been proposed.
7.	Accessing Complex Tetrahydrofurobenzo-Pyran/Furan Scaffolds via Lewis-Acid Catalyzed Bicyclization of Cyclopropane Carbaldehydes with Quinone Methides/Esters N Kaur, P Kumar, S Dutt, P Banerjee – The Journal of Organic Chemistry, 2022 **Abstract:** Herein, we report a straightforward one-pot synthesis of tetrahydrofurobenzopyran and tetrahydrofurobenzofuran systems via an in situ ring-expansion of the cyclopropane carbaldehydes followed by a [2 + n] cycloaddition with the quinone derivatives. The transformation not only unveils a new reaction mode of cyclopropane carbaldehydes with quinone methides/esters, but also promotes a step-efficient diastereoselective route to the sophisticatedly fused oxygen tricycles that can be further dehydrogenated to access the valued dihydro-2H-furo[2,3-b]chromene frameworks. 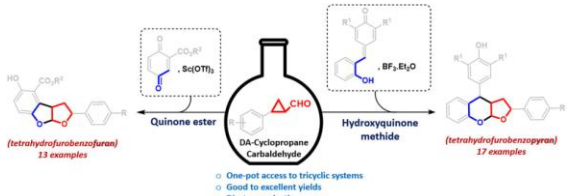
8.	An Unconventional Measurement Technique to Estimate Power Transfer Efficiency in Series–Series Resonant WPT System Using S-Parameters A Bharadwaj, A Sharma, CC Reddy – IEEE Transactions on Instrumentation and Measurement, 2022 **Abstract:** Power transfer efficiency is a critical performance parameter for the coil design of a wireless power transfer (WPT) system. An accurate and simplistic measurement technique of power transfer efficiency will ensure the system less susceptible to the external environment with high reliability. Broadly, S-parameter-based efficiency is considered a precise measurement technique attained by the network analyzer. However, it lacks consistency in the practical scenario, the input–output ports being calibrated at 50 Ω . Accordingly, most of the power dissipates in the instrument's internal resistance. Therefore, this article proposes a novel S-parameter efficiency measurement technique aided by user-calibrated source and load factors. This technique's output ensures the WPT system's performance assessment even at high frequencies by S-parameters at all conditions. Besides, the proposed technique is experimentally verified and compared with various conventional techniques employed in several literary works.
9.	Bifunctional Acid-base Zirconium Phosphonate for Catalytic Transfer Hydrogenation of Levulinic acid and Cascade Transformation of Furfural to Biofuel Molecules AK Manal, JH Advani, R Srivastava – ChemCatChem, 2022 **Abstract:** The production of biofuels, such as furfural ether and γ-valerolactone (GVL) from biomass platform chemicals furfural (FFA) and Levulinic acid (LA) is of significant interest. In

	this study, a nanoporous inorganic-organic Zr-phosphonate catalyst was synthesized and employed in the selective production of GVL (98.2%) via catalytic transfer hydrogenation of LA. The catalyst containing acid-base sites was further used to produce biofuel molecules like GVL and furfuryl ether under a mild reaction condition via cascade furfural transformation. The GVL selectivity was further improved using phosphotungstic acid/ZrNPO 3 . The catalytic optimization studies were combined with poisoning studies and the detailed physicochemical characterization to acquire insight into the structure-activity correlation and reaction mechanism. The synergistic presence of the Lewis acidity and basicity on the catalyst was responsible for its remarkable activity. Designing a single catalyst for the one-pot tandem transformation of FFA to GVL would be highly motivating for catalysis researchers and industrialists. 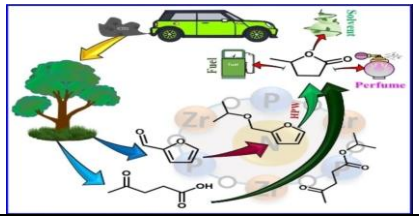
10.	Computationally inexpensive semi-analytical thermal model to predict melt-pool dimensions for a single-track in Selective Laser Melting SK Nandi, R Kumar, A Agrawal – Journal of Manufacturing Processes, 2022 **Abstract:** Selective laser melting (SLM) has recently gained momentum as a state-of-the-art manufacturing process capable of building highly customized products. Localized heat input and short interaction time of laser beam intensify thermal gradient and deteriorate the part's quality due to thermal stresses and uncontrolled distortions. An algorithm is proposed that comprises of analytical solution for volumetric moving heat source combined with numerically formulated conduction and convection cooling to estimate the temperature distribution and melt-pool geometry during the SLM process. Fully implicit finite volume equations are framed with appropriate part boundary conditions for the two-dimensional domain and iteratively solved by Alternating Direction Implicit (ADI) method. The proposed methodology has shown the potential to develop a deep understanding of this dynamic process and deliver results at low computational costs. Simulations for single-track melting have been studied by changing the process parameters, and phase change from powder to solid is well exhibited by adopting temperature-dependent material properties. The proposed model has been validated by experimental data from the literature for two alloys - Inconel 718 and SS316L. **Graphical Abstract:** 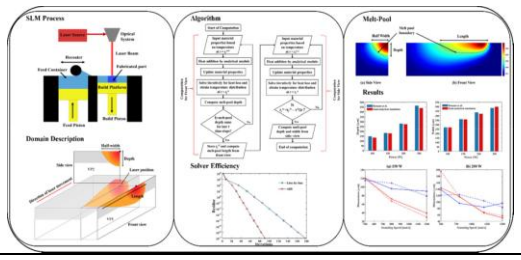
11.	Configurational force based analysis of creep crack growth O Kolednik, A Tiwari, C Posch, M Kegl – International Journal of Fracture, 2022 **Abstract:** Based on the concept of configurational forces, the driving force of cracks in elastic–plastic, creeping materials is derived. In a numerical study, the variation of the crack driving force with increasing creep time is compared to the behaviors of different parameters that have been used in literature to describe the tendency to creep crack growth. This is performed for the assumption of stationary cracks in C(T)-specimens made of Waspaloy at 700 °C. The loading

	conditions are varied so that small-scale creep, transition creep, or extensive creep conditions prevail. Either the load or the load-point displacement are held constant. It is demonstrated that, for the considered cases, the conventional creep crack growth parameters do not reflect the crack driving force, but qualitatively follow a behavior similar to the (absolute value of the) time derivative of the crack driving force.
12.	Copper nanoparticles embedded in polyaniline derived nitrogen-doped carbon as electrocatalyst for bio-energy generation in microbial fuel cells SK Dhillon, A Chaturvedi, D Gupta, TC Nagaiah.. – Environmental Science and Pollution Research, 2022 **Abstract:** Microbial fuel cells (SC-MFCs) have emerged as green energy devices to resolve the growing energy and environmental crisis. However, the technology's application depends on the sluggish oxygen reduction reaction (ORR) kinetics. Among the electrocatalysts explored, transition metal-nitrogen-carbon composites exhibit satisfactory ORR activity. Herein, we investigate the performance of copper-nitrogen-carbon (Cu/NC) electrocatalysts for ORR, highlighting the effect of temperature, role of nitrogen functionalities, and Cu–N_x sites in catalyst performance. Cu/NC-700 demonstrated satisfactory ORR activity with an onset potential of 0.7 V (vs. RHE) and a limiting current density of 3.4 mA cm^{-2}. Cu/NC-700 modified MFC exhibited a maximum power density of 489.2 mW m^{-2}, higher than NC-700 (107.3 mW m^{-2}). These observations could result from synergistic interaction between copper and nitrogen atoms, high density of Cu–N_x sites, and high pyridinic-N content. Moreover, the catalyst exhibited superior stability, implying its use in long-term operations. The electrocatalytic performance of the catalyst suggests that copper-doped carbon catalysts could be potential metal-nitrogen-carbon material for scaled-up MFC applications.
13.	Deep Learning based Detection of Foot Lift Event Using a Single Accelerometer for Accurate Firing of FES B Basumatary, R Suvra Halder & A Sahani – Sensing Technology, 2022 **Abstract:** Foot drop (FD) is defined as the inability to lift the front part of the foot from the ground. It can be corrected by functional electrical stimulation (FES) of the peroneal nerve by applying pulses of a given duration, amplitude, and frequency. For correcting the FD through FES, it requires accurate detection of the foot lift event (gait pattern) of the patient. The stimulation pulse of FES device has to be triggered only when the subject is trying to lift the foot. In a traditional FES system, foot lift is detected by sensor attached below the heel. However, such type of sensor requires cables which create discomfort to the patient while wearing the device. To avoid this cable complexity, different types of Inertial Measurement Unit (IMU) based sensors are used. However, those types of IMU based sensors have some disadvantages, such as false triggering, and still, there is a lack of a proper algorithm to detect proper foot lift event by the sensor. In this paper, we have proposed a Deep learning based foot lift detection algorithm using a single accelerometer. Our proposed algorithm has been implemented in our developed FES device, and it was successful in predicting the foot lift event.
14.	Drug eluting titanium implants for localised drug delivery M Singh, AS Gill, PK Deol, A Agrawal, SS Sidhu – Journal of Materials Research, 2022 **Abstract:** Titanium and its alloys are considered as one of the mainstream materials for fabricating orthopaedic and dental implants. In spite of their satisfactory success rate, implant failure is reported in terms of poor osseointegration, bone resorption and postsurgical infections. Localised drug delivery through implant has gained immense interest due to its flexibility in delivering different drugs directly to target site and addressing dose-related adverse effects. Surface modification through coating or adsorption is used to fabricate drug eluting titanium implants. Currently two approaches are in use. First involves modification of implant surface or pores with drug loaded carrier (polymers, ceramics, or composite). Other is to load drug to the

	implant material itself without drug carrier. Controlled drug release and mechanical and physical stability of coated or adsorbed materials are the major researched areas. Review discusses the current advancements in both the approaches for developing multifunctional titanium implants for localised drug delivery. **Graphical Abstract:** 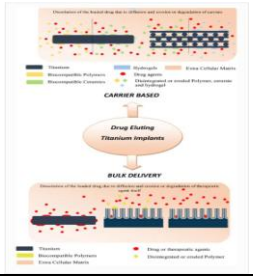
15.	EEG-ConvTransformer for single-trial EEG-based visual stimulus classification S Bagchi, DR Bathula – Pattern Recognition, 2022 **Abstract:** Different categories of visual stimuli evoke distinct activation patterns in the human brain. These patterns can be captured with EEG for utilization in application such as Brain-Computer Interface (BCI). However, accurate classification of these patterns acquired using single-trial data is challenging due to the low signal-to-noise ratio of EEG. Recently, deep learning-based transformer models with multi-head self-attention have shown great potential for analyzing variety of data. This work introduces an EEG-ConvTranformer network that is based on both multi-headed self-attention and temporal convolution. The novel architecture incorporates self-attention modules to capture inter-region interaction patterns and convolutional filters to learn temporal patterns in a single module. Experimental results demonstrate that EEG-ConvTransformer achieves improved classification accuracy over state-of-the-art techniques across five different visual stimulus classification tasks. Finally, quantitative analysis of inter-head diversity also shows low similarity in representational space, emphasizing the implicit diversity of multi-head attention.
16.	Effect of turbidity on choice of zonal thicknesses in solar ponds under various performance evaluation criteria S Verma, R Das – Journal of Cleaner Production, 2022 **Abstract:** A turbid solar pond is investigated to study how turbidity in the insulating zone affects the optimum dimensions of the pond, that suit a concerned design criterion. Four different criteria for the optimization have been undertaken, namely: minimizing the maturation time period, maximizing the extraction power under no constraint, maximizing the extraction power under constraint of fixed pond volume and maximizing the extraction power while simultaneously minimizing the volume. Transient numerical solution is sought for the first criterion, whereas for remaining three, a steady-state analytical model is employed that assesses the year-round extraction performance. Simplified versions of the respective models have been validated with data obtained experimentally and with theoretical data available in the literature. It is revealed that turbidity in the salinity gradient zone can lead to considerable alterations in the optimal pond dimensions, regardless of what the criterion used for optimization. The maximum errors in the optimal insulating zone and heat storage zone thickness values, arising from neglect of turbidity are observed to be about 125% and 60%, respectively. Hence, either attempts should be made to make solar ponds free of any foreign agents that cause turbidity, or if not, then they should be designed considering this factor into account, for which this work can serve as a guiding study. **Graphical Abstract:**

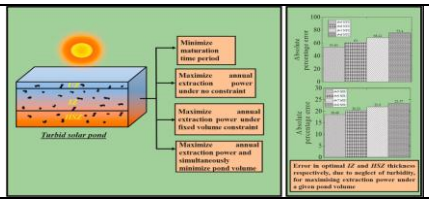

17. [Effects of intake charge temperature and relative air-fuel ratio on the deterministic characteristics of cyclic combustion dynamics of a HCCI engine]
A Singh, RK Maurya – International Journal of Engine Research, 2022

Abstract: Homogenous charge compression ignition (HCCI) combustion can significantly reduce automotive pollution and increase the thermal efficiency of the engine. However, combustion phasing control is a major challenge in HCCI engines due to severe cyclic combustion variations. This study investigates the cyclic combustion dynamics of the HCCI engine using nonlinear dynamic methods such as return maps, recurrence plots (RPs), and recurrence quantitative analysis (RQA). Combustion stability and cyclic variations of HCCI combustion parameters were investigated on a modified four-stroke diesel engine. The experiments were conducted by varying relative air-fuel ratios (λ) and intake air temperatures (TiTi) at two engine speeds. In-cylinder pressure data of 2000 consecutive engine combustion cycles is logged for each test condition. In this study, deterministic characteristics of combustion phasing (CA_{50}) and crank angle position of maximum cylinder pressure (θPmaxθPmax) are investigated and compared by employing nonlinear dynamical methods. Return maps revealed that θPmaxθPmax is having distinct and more frequently observed deterministic characteristics in comparison to CA_{50}. Patterns in RPs showed a more persistent and sudden change in the combustion dynamics at higher engine speeds. Recurrence plot-based analysis found the existence of deterministic features in the combustion dynamics irrespective of the operating conditions. It was found using RQA parameters that the deterministic nature becomes stronger with a decrease in TiTi and any deviation in intermediate values of λ. Additionally, RQA measures advocate that CA_{50} has more deterministic characteristics at higher engine speed while θPmax at lower engine speed. Strong coupling and synchronization between θPmax and CA_{50} is indicated by cross-recurrence plots and CPR index when engine operated with a comparatively richer mixture.

18. [Enhanced reversible hydrogen storage efficiency of zirconium-decorated biphenylene monolayer: A computational study]
P Mane, SP Kaur, B Chakraborty – Energy Storage, 2022

Abstract: Metal decorated carbon-containing two-dimensional monolayers have been explored as potential hydrogen storage materials because of their open structures which improve the storage capacity. Here, the H2 storage capability of the Zr-decorated biphenylene nanosheet is studied with the aid of first-principles calculations. Biphenylene is a recently synthesized ultra-flat material consisting of different-sized carbon rings. Zr atom interacts strongly with the monolayer with a binding energy of −4.79 eV due to charge transfer from Zr 3d orbital to C-2p orbital of biphenylene nanosheet. The hydrogen molecules bind to the Zr-decorated biphenylene monolayer with an average adsorption energy of −0.4 eV per H2 due to Kubas-type interactions involving charge transfer between metal d orbital and H-1s orbital. The Zr decoration helps to adsorb up to 9 hydrogen molecules per metal atom on the monolayer resulting in the H2 uptake of 9.95 wt%, higher than the target of 6.5 wt% set by the Department of Energy (DoE), USA. The high diffusion barrier for the Zr atom prevents metal-metal clustering. The ab initio molecular dynamics (AIMD) simulations show that the complexes remain stable even at the highest desorption temperature. The present study shows that the Zr-decorated biphenylene can be considered a prospective two-dimensional material for reversible hydrogen storage.

19. [Exosomal Transfer of DNA Methyl-Transferase mRNA Induces an Immunosuppressive

	Phenotype in Human Monocytes JR Wisler, K Singh, A McCarty, R Harkless, D Mukherjee.. – Shock (Augusta, Ga.), 2022 **Abstract:** Introduction Survivors of sepsis exhibit persistent immunosuppression. Epigenetic events may be responsible for some of these immunosuppressive changes. During sepsis circulating exosomes contain large quantities of DNA methyltransferase (DNMT) mRNAs. We hypothesized that exosomes directly transfer DNMT mRNAs to recipient monocytes with resultant methylation events and immunosuppression. Methods Exosomes containing DNMT mRNA were generated by stimulating monocytes with LPS. Confocal microscopy was used to determine uptake kinetics in the presence of pharmacologic inhibition. Expression and packaging of specific DNMT mRNA was controlled using DNMT siRNAs. Whole genome and gene specific methylation was assessed using bisulfite sequencing. Ingenuity pathway analysis was performed to determine the biological function of significance of differentially methylated regions. Results Exosomes effectively transferred DNMT mRNA to recipient monocytes. Pharmacologic inhibition of exosome uptake prevented this increase in DNMT mRNA expression. Recipient monocytes exhibited hypermethylation changes and gene suppression. siRNAs decreased the packaging of DNMT mRNAs and prevented TNFα gene suppression, restoring immunocompetence. Conclusion These data support a role for exosome-mediated transfer of DNMT mRNA with resultant methylation and gene silencing. Pharmacologic uptake inhibition or targeted siRNA mediated DNMT gene silencing prevented DNMT mRNA transfer and maintained the cell's ability to express TNFα in response to LPS. This highlights the potential therapeutic value of targeting these exosome-mediated epigenetic events to maintain the host immune response during sepsis.
20.	Expectation-Maximization Algorithm for Autoregressive Models with Cauchy Innovations MS Dhull, A Kumar – Engineering Proceedings, 2022 **Abstract:** In this paper, we study the autoregressive (AR) models with Cauchy distributed innovations. In the AR models, the response variable yt depends on previous terms and a stochastic term (the innovation). In the classical version, the AR models are based on normal distribution which could not capture the extreme values or asymmetric behavior of data. In this work, we consider the AR model with Cauchy innovations, which is a heavy-tailed distribution. We derive closed forms for the estimates of parameters of the considered model using the expectation-maximization (EM) algorithm. The efficacy of the estimation procedure is shown on the simulated data. The comparison of the proposed EM algorithm is shown with the maximum likelihood (ML) estimation method. Moreover, we also discuss the joint characteristic function of the AR(1) model with Cauchy innovations, which can also be used to estimate the parameters of the model using empirical characteristic function.
21.	Exploiting Heteroaggregation to Quantify the Contact Angle of Charged Colloids at Interfaces M Sabapathy, KZ Md, H Kumar, S Ramamirtham.. – Langmuir, 2022 **Abstract:** We exploit the aggregation between oppositely charged particles to visualize and quantify the equilibrium position of charged colloidal particles at the fluid–water interface. A dispersion of commercially available charge-stabilized nanoparticles was used as the aqueous phase to create oil–water and air–water interfaces. The colloidal particles whose charge was opposite that of the nanoparticles in the aqueous phase were deposited at the chosen fluid–water interface. Heteroaggregation, i.e., aggregation between oppositely charged particles, leads to the

	deposition of nanoparticles onto the larger particle located at the interface; however, this only occurs on the surface of the particle in contact with the aqueous phase. This selective deposition of nanoparticles on the surfaces of the particles exposed to water enables the distinct visualization of the circular three-phase contact line around the particles positioned at the fluid–water interface. Since the electrostatic association between the nanoparticles and the colloids at interfaces is strong, the nanoparticle assembly on the larger particles is preserved even after being transferred to solid substrates via dip-coating. This facilitates the easy visualization of the contact line by electron microscopy and the determination of the equilibrium contact angle of colloidal particles (θ) at the fluid–water interface. The suitability of the method is demonstrated by the measurement of the three-phase contact angle of positively and negatively charged polystyrene particles located at fluid–water interfaces by considering particles with sizes varying from 220 nm to 8.71 μm. The study highlights the effect of the size ratio between the nanoparticles in the aqueous phase and the colloidal particles on the accuracy of the measurement of θ. **Graphical Abstract:** 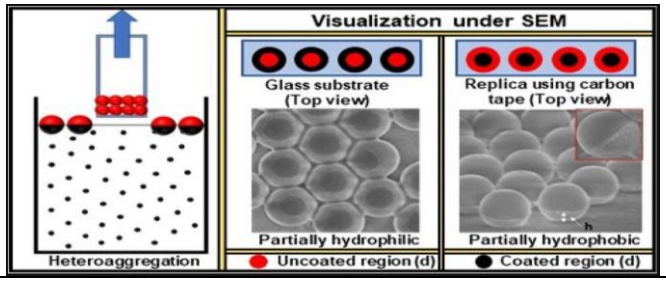
22.	First record of insectivore from the late Oligocene, Kargil Formation (Ladakh Molasse Group), Ladakh Himalayas WA Wazir, F Cailleux, RK Sehgal, R Patnaik, N Kumar.. – Journal of Asian Earth Sciences: X, 2022 **Abstract:** The Kargil Formation in the region of Ladakh (northern India) is known for its late Oligocene mammal fauna of both large mammals and rodents. New excavations in the area yielded a maxillary fragment of an insectivore with three premolars and two roots of a canine. The fossil record of the insectivores on the Indian subcontinent is as yet scanty. Based on the peculiar morphology of the last premolar, the Ladakh fossil could be identified as belonging to a new species of Erinaceinae, Ladakhechinus iugummontis n. gen. n. sp. The new find confirms the large diversity among hedgehogs in Asia during the Oligocene.
23.	Fracture in self-lubricating inserts: A case study A Pratap, BK Singh, N Sardana – Materials Today: Proceedings, 2022 **Abstract:** A case study is carried out to reveal the fracture mechanism of self-lubricating inserts. The insert is made up of 98.5 wt% Zirconia Toughened Alumina (ZTA) reinforced with 1.5 wt% CuO. The insert is fabricated through the powder metallurgy route, followed by the hot isostatic pressing (HIP) technique (for densification). After densification, the insert is shaped and sized according to ISO SNUN 120408. The workpiece material used for machining is AISI 4340 steel. A conventional NH-26 lathe is used for machining as well as for creating facture inside the insert. In this investigation, the machining operations are carried out till the failure of inserts does not take place. The fracture analysis suggested a synonymous fracture mechanism that occurs for brittle facture (facture without any deformation). The fracture analysis seen through FESEM images observed that the initiation of crack that happened without any dislocation movement results in chipping, cracking, and flaking on the surface. The crack is initialized due to the generation of high localized stresses. The stresses were developed due to the continuous movement of chips concentrated slightly away from the cutting edges. The developed stresses

	are relieved by creating small cracks beneath the surface. These cracks are propagated in the radial direction without any dislocation-induced plasticity. The mechanism is well confirmed through the FESEM images of fracture specimens.
24.	Generic Multispectral Demosaicking Based on Directional Interpolation V Rathi, P Goyal – IEEE Access, 2022 **Abstract:** The low-cost snapshot multispectral spectral imaging systems with multispectral filter array (MSFA) require generic MSFA demosaicking methods to generate the multispectral image (MSI) with a variable number of spectral bands depending on the applications. Most of the existing MSFA demosaicking methods are either non-generic or perform inadequately. This paper presents a new generic MSFA demosaicking method based on the directional weighted interpolation. Our proposed method calculates the four directional estimates around the location of the unknown pixel and combines them in a weighted manner using the local edge magnitude in the corresponding directions to estimate the missing pixel values. Experimental results confirm that the proposed demosaicking method provides improvement, compared to the state-of-the-art generic demosaicking methods in terms of both subjective and objective evaluations on the two benchmark MSI datasets. 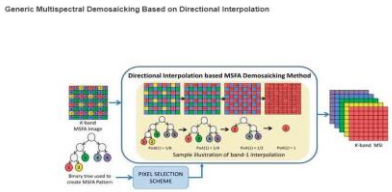
25.	High-performance aqueous sodium-ion/sulfur battery using elemental sulfur M Kumar, N Thakur, A Bordoloi, AK Yadav, SN Jha, D Bhattacharyya, D Mandal, TC Nagaiah – Journal of Materials Chemistry A, 2022 **Abstract:** Despite a promising outlook, the large-scale application of aqueous rechargeable sodium-ion batteries (ARSIBs) was impeded due to low-capacity electrode materials. Herein, we report a high capacity elemental sulfur-anode (S@NiVP/Pi-NCS) for aqueous rechargeable sodium ion/sulfur batteries using 70% of elemental sulfur, which delivers an outstanding capacity of 826 mA h g^{-1} at 0.5C with an excellent cycling stability even at 10C and a negligible capacity decay with 0.03% sulfur loss per cycle even after 400 cycles. The NiVP/Pi-NCS host combines the merits of fast anchoring and high conductivity of the composite to achieve smooth anchoring-diffusion and conversion of sodium polysulfide. The superior anchoring and accelerated polysulfides redox kinetics were confirmed by various electrochemical studies and in situ spectro-electrochemical analysis. Chemical interaction with vanadium provides faster redox kinetics of polysulfide conversion and efficient anchoring as revealed by XPS and was further supported by XANES and EXAFS studies wherein the distortion at the V site and overlapping electronic states in the NiVP/Pi catalyst were observed. Further, a full cell battery assembled using S@NiVP/Pi-NCS anode and $Na_{0.44}MnO_2$ cathode demonstrates an excellent initial capacity of 756 mA h g^{-1} based on S loading and 98.3 mA h g^{-1} based upon total electrode weight with 95% of capacity retention even after 600 cycles and a remarkable energy density of 84 W h kg^{-1} at 0.5C. Two full cells connected in series able to power LED demonstrate its practical application. 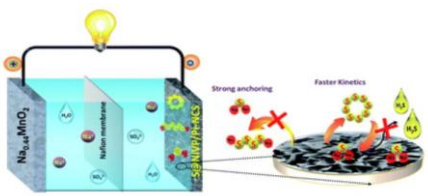

26.	Improving the Glucose to Fructose Isomerization via Epitaxial-Grafting of Niobium in UIO-66 framework AK Kar, R Srivastava – ChemCatChem, 2022 **Abstract:** Glucose to fructose transformation is an essential transformation for the success of biorefinery. Herein, the epitaxial-grafting of Nb in UIO-66 significantly improved the fructose yield. Post-synthesis incorporating Nb in the UIO-66 phenomenally improved the glucose conversion from 31.1 % to 71.8 % and fructose selectivity from 38.2 % to 71.2 %. The incorporation of Nb was confirmed from the FTIR, HR-TEM investigation, EDX analysis, and elemental mapping. The XPS analysis distinctly stated the successful incorporation of Nb and generation of Zr-O-Nb oxo clusters in the UIO-66 framework. The NH 3 -TPD provided distinguishable information about the chemical interaction of Nb with the UIO-66 framework that resulted in the increase of the acid strength after the Nb incorporation in the UIO-66 catalyst. The content of Nb and reaction parameters, especially temperature and duration, control the glucose to fructose isomerization over glucose to mannose epimerization. The structure-activity relationship was established, and a reaction mechanism was proposed. The catalyst was recycled five times with only a low decrease in the fructose yield (47.3 % to 42.2 %) than several reported MOFs catalysts. The activity of the developed catalyst was higher or similar to the reported catalysts. The successful grafting of Nb demonstrates that by swiftly modifying the acidity of the catalyst, a superior activity can be achieved. 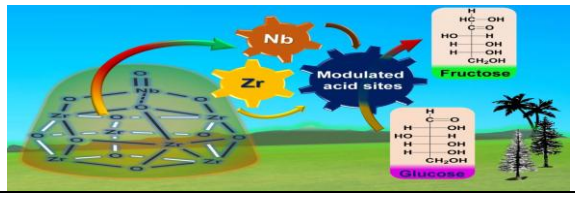
27.	Integrated Power Converter with G2V, V2G and Direct V2V Capabilities for SRM Drive Based Electric Vehicle Application V Shah, G Kumawat, S Payami – ICPC2T 2022 - 2nd International Conference on Power, Control and Computing Technologies, Proceedings, 2022 **Abstract:** The article presents the design and implementation of an integrated power converter (IPC) for a switched reluctance motor (SRM) drive based electric vehicle (EV) application. The IPC proposed integrates driving and battery energy storage (BES) charging/discharging functionality. During BES charging mode, i.e., grid-To-vehicle (G2V) charging, the proposed IPC is reutilized as a bridgeless boost power factor correction circuit (PFCC) in cascade with a bidirectional DC-DC converter (BDDC). Similarly, during BES discharging mode, i.e., vehicle-To-grid (V2G) charging, the proposed IPC is reutilized as a BDDC in cascade with a single-phase voltage source inverter. Thus, with the proposed IPC, the BES can be charged/discharged at AC grid voltage. The proposed IPC also supports DC fast/vehicle-To-vehicle (V2V) charging wherein the host EV via the integrated BDDC can charge/discharge a receiver EV of higher or lower BES voltage rating than the host EV. In addition, during G2V, V2G and V2V charging, the charging current flowing in phase winding/s when reconfigured as charging inductor/s results in a zero-Torque production. Detailed theoretical analysis and experimental verification on a prototype 4-phase SRM are presented to evaluate the proposed IPC's driving and BES charging features.
28.	Ionic Liquid-Mediated One-Pot 3-Acylimino-3H-1,2-dithiole Synthesis from Thiocarboxylic Acids and Alkynylnitriles via In Situ Generation of Disulfide Intermediates C Kumari, A Goswami – The Journal of Organic Chemistry, 2022 **Abstract:** A practical and straightforward strategy for the synthesis of 3-acylimino-3H-1,2-dithiol derivatives via a metal-free annulation reaction of alkynylnitriles with thiocarboxylic

	acids mediated by ionic liquids [BMIM]Br has been reported. This operationally simple protocol offers an easy and rapid access to a library of dithiol derivatives in moderate to good yields. The mechanistic studies show a benzoyldithio anion addition to alkynylnitriles followed by an annulation reaction through the involvement of a disulfide moiety as the key intermediate. 
29.	Lewis Acid-Assisted Transition Metal-Free Aminocyanation of Alkynes with Arylamines and N-Cyanosuccinimide I Chatterjee, G Kumar, D Bhattacharya – Advanced Synthesis & Catalysis, 2022 **Abstract:** A transition-metal-free aminocyanation of aryl alkynes has been achieved using indium tribromide, $InBr_3$ or $B(C_6F_5)_3$ as a Lewis acid. This aminocyanation protocol features with non-toxic cyanide source, a good substrate scope and potentially valuable aminocyanation products. Mechanistic studies reveal the complex formation between Lewis acid and alkyne to produce in situ alkyne nitrile as a key intermediate. Further hydroamination of alkyne nitrile with arylamines affords the E-selective (E:Z=70:30 to 90:10) β-aminoacrylonitrile derivatives.
30.	$Ln_2Te_6O_{15}$ (Ln = La, Gd, and Eu) "Anti-Glass" Phase-Assisted Lanthanum-Tellurite Transparent Glass–Ceramics: Eu^{3+} Emission and Local Site Symmetry Analysis P Patra, R Kumar, K Jayanthi, M Fábián, G Gupta… – Inorganic Chemistry, 2022 Abstract: The presence of lanthanide-tellurite "anti-glass" nanocrystalline phases not only affects the transparency in glass–ceramics (GCs) but also influences the emission of a dopant ion. Therefore, a methodical understanding of the crystal growth mechanism and local site symmetry of doped luminescent ions when embedded into the precipitated "anti-glass" phase is crucial, which unfolds the practical applications of GCs. Here, we examined the $Ln_2Te_6O_{15}$ "anti-glass" nanocrystalline phase growth mechanism and local site symmetry of Eu^{3+} ions in transparent GCs produced from $80TeO_2–10TiO_2–(5 – x)La_2O_3–5Gd_2O_3–xEu_2O_3$ glasses, where x = 0, 1, 2. A crystallization kinetics study identifies a unique crystal growth mechanism via a constrained nucleation rate. The extent of "anti-glass" phase precipitation and its growth in GCs with respect to heat-treatment duration is demonstrated using X-ray diffraction (XRD) and field emission scanning electron microscopy (FE-SEM) analysis. Qualitative analysis of XRD confirms the precipitation of both $La_2Te_6O_{15}$ and $Gd_2Te_6O_{15}$ nanocrystalline phases. Rietveld refinement of powder X-ray diffraction patterns reveals that Eu^{3+} ions occupy "Gd" sites in $Gd_2Te_6O_{15}$ over "La" sites in $La_2Te_6O_{15}$. Raman spectroscopy reveals the conversion of TeO_3 units to TeO_4 units with Eu_2O_3 addition. This confirms the polymerizing role of Eu_2O_3 and consequently high crystallization tenacity with increasing Eu_2O_3 concentration. The measured Eu^{3+} ion photoluminescence spectra revealed its local site symmetry. Moreover, the present GCs showed adequate thermal cycling stability (~50% at 423 K) with the highest activation energy of around 0.3 eV and further suggested that the present transparent GCs would be a potential candidate for the fabrication of red-light-emitting diodes (LEDs) or red component phosphor in W-LEDs. 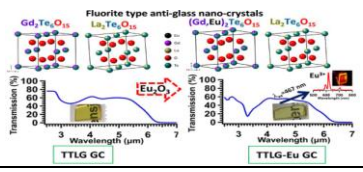
31.	MAPCP: Memory Access Pattern Classifying Prefetcher MM Jamadar, J Kaur, S Das – ACM International Conference Proceeding Series, 2022 **Abstract:** Prefetching is a technique used to improve system performance by bringing data or

	instructions in the cache before it is demanded by the core. Several prefetching techniques have been proposed, in both hardware and software, to predict the data to be prefetched with high accuracy and coverage. The memory patterns accessed by applications can be classified as either regular memory access patterns or irregular memory access patterns. Most prefetchers exclusively target either of these patterns by learning from either temporal or spatial correlation among the past data accesses observed. Our proposal focuses on covering all kinds of access patterns which can be predicted by a temporal as well as a spatial prefetcher. Running both kinds of prefetchers in parallel is not a wise design as it leads to unnecessary hardware (storage) overhead for metadata storage of temporal prefetcher. We propose broadly classifying the memory access patterns of applications on the go as regular or irregular, and then using an appropriate prefetcher to issue prefetches for the respective classes. This reduces the metadata requirement in case of temporal prefetcher by 75%. Evaluation of our proposed solution on SPEC CPU 2006 benchmarks achieve a speedup of 23.7% over the no-prefetching baseline, which is a 4% improvement over the state of the art spacial prefetcher BIP, and 13.2% improvement over the temporal prefetcher, Triage.
32.	Muscle weakness assessment tool for automated therapy selection in elbow rehabilitation S Gupta, A Agrawal, E Singla – Robotica, 2022 **Abstract:** Clinical observations and subjective judgements have traditionally been used to evaluate patients with muscular and neurological disorders. As a result, identifying and analyzing functional improvements are difficult, especially in the absence of expertise. Quantitative assessment, which serves as the motivation for this study, is an essential prerequisite to forecast the task of the rehabilitation device in order to develop rehabilitation training. This work provides a quantitative assessment tool for muscle weakness in the human upper limbs for robotic-assisted rehabilitation. The goal is to map the assessment metrics to the recommended rehabilitation exercises. Measurable interaction forces and muscle correlation factors are the selected parameters to design a framework for muscular nerve cell condition detection and appropriate limb trajectory selection. In this work, a data collection setup is intended for extracting muscle intervention and assessment using MyoMeter, Goniometer and surface electromyography data for upper limbs. Force signals and human physiological response data are evaluated and categorized to infer the relevant progress. Based upon the most influencing muscles, curve fitting is performed. Trajectory-based data points are collected through a scaled geometric Open-Sim musculoskeletal model that fits the subject's anthropometric data. These data are found to be most suitable to prescribe relevant exercise and to design customized robotic assistance. Case studies demonstrate the approach's efficacy, including optimally synthesized automated configuration for the desired trajectory.
33.	Near Data Processing and Its Applications Angelic, M Mahobe, J Kaur, S Das – Soft Computing: Theories and Applications, 2022 **Abstract:** There has been a gradual shift from traditional computing to technologies involving more data-centric architectures. This has led to tremendous growth in the amount of data and, furthermore, the data-intensive applications. The major bottleneck with such applications is the data movement that is required between memory/storage and CPU. To improve the performance of such applications and reduce the movement of data from memory to CPU for computation, near data processing (NDP) is the alternative, which moves the computation from CPU to memory. This helps to improve performance, utilize bandwidth properly and reduce energy consumption to a great extent, which helps to execute data-intensive applications efficiently. In this paper, we have discussed the basics of NDP and the methods which have been proposed for the implementation of NDP. We have also discussed the applications that require NDP for better performance.
34.	Novel sustainable cryo-lubrication strategies for reducing tool wear during ultrasonic-assisted turning of Inconel 718

	N Khanna, J Airao, CK Nirala, GM Krolczyk – Tribology International, 2022 **Abstract:** This paper deals with the concerns of industrial demand for enhancing the machinability of Inconel 718. In this regard, sustainable cooling strategies, i.e., minimum quantity lubrication (MQL), electrostatic minimum quantity lubrication (EMQL), and liquid carbon dioxide (LCO2), in combination with ultrasonic-assisted turning, are used to reduce the tool wear in the machining of Inconel 718. An in-house developed ultrasonic-assisted turning setup is used to perform the experiments. Six different combinations of cooling strategies are used to perform the experiments. These cooling strategies are LCO2 +MQL (in this case LCO2 is used on the rake face and MQL on the flank face of the tooling), MQL+LCO2, EMQL+LCO2, LCO2+EMQL, EMQL+MQL, and MQL+EMQL. The results show that the electrostatic minimum quantity lubrication provided on the flank face and the liquid carbon dioxide provided on the rake face considerably reduce the tool wear, power consumption, and specific cutting energy without hindering the surface quality. Thus, the novel combination of liquid carbon dioxide and electrostatic minimum quantity lubrication attains sustainability in machining Inconel 718. **Graphical Abstract:** 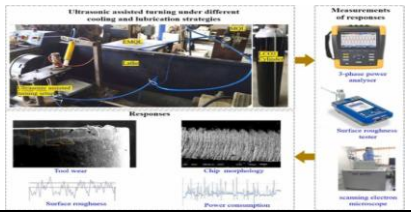
35.	Optimal Selection of Voltage Controlling Parameter in Uncertain Active Distribution Network D Kumar, B Prasad – 2022 4th International Conference on Energy, Power and Environment (ICEPE), 2022 **Abstract:** Nowadays, the penetration of converter base Generation (CBG) is increasing rapidly in the distribution system. Thus, maintaining the voltage profile of the distribution system becomes a challenging issue due to the uncertain nature of renewable sources. Therefore, in this paper, the voltage profile is improved by choosing optimal voltage controlling parameters. This is achieved through a multi-objective optimal power flow in a distribution system with CBG like solar and wind power. Further, the Modified Jaya (M-Jaya) algorithm has been used to solve the optimization by converting multi objectives, such as minimization of line losses, minimization of voltage deviation and maximization of CBG output power to a single objective function. Moreover, the state-based probabilistic model has been formulated for CBG output power, which gives the probability of all possible output power from DGs for any specific time period. The numerical test of the multi-objective optimal power flow with the proposed state-based probabilistic generation model has been done on enhanced the IEEE-33 test system.
36.	Parameter Identification in Population Balance Models Using Uncertainty and Sensitivity Analysis P Sehrawat, D Sarkar, J Kumar – Industrial & Engineering Chemistry Research, 2022 **Abstract:** The accurate estimation of sensitive parameters in a mathematical model predicting the outcome of a real experiment is of great importance in studying a complex physical phenomenon. A systematic methodology based on the uncertainty and sensitivity analysis framework is proposed for precise estimation of model parameters. The nonintrusive polynomial chaos expansion and the Sobol'-based sensitivity indices are used to quantify the uncertainties in the model prediction due to parameter uncertainties, and the Monte Carlo method is used for the validation of uncertainty quantification results. A population balance model for an unseeded batch cooling crystallization of l-asparagine monohydrate with two different sets of kinetic

	models for nucleation and crystal growth is selected to demonstrate the methodology. The results clearly demonstrate the effectiveness of the proposed strategy in improving the predictive ability of the population balance model. For models involving many uncertain parameters, the proposed strategy can be adopted to rank parameters by decreasing importance and then achieve precise estimation of the more significant parameters using a suitable optimization algorithm and experimental data set. **Graphical Abstract:** 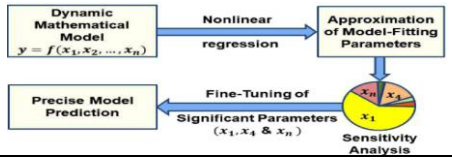
37.	Polymeric Lipid Nanoparticles for Donepezil Delivery M Bhandari, N Rasool, Y Singh – Lecture Notes in Bioengineering, 2022 **Abstract:** Donepezil hydrochloride, an anticholinesterase drug, is orally administered to patients suffering from Alzheimer's disease. Alzheimer's is a neurodegenerative disorder characterized by the degradation of neurotransmitters, neuronal apoptosis, and loss of synapses. The treatment of such neural diseases is hampered by the presence of a tightly controlled blood–brain barrier (BBB), which prevents the influx of drugs. The intranasal route of drug delivery has been lately seen as a promising approach to deliver drugs directly to the brain, effectively bypassing the BBB, as it offers high absorption and increased bioavailability. In this study, we have fabricated hybrid polymeric lipid nanoparticles with two natural polymers—chitosan and gelatin. The average particle sizes of chitosan lecithin and gelatin lecithin nanoparticles were 237.43 and 278.86 nm. The percentage drug loading for chitosan lecithin and gelatin lecithin nanoparticles was 10.24 ± 0.4 and 8.77 ± 0.748%. The chitosan lecithin nanoparticles showed a burst release of up to 99.99% drug for 5 days, while the gelatin lecithin nanoparticles exhibited a sustained release of 33.31% drug for 30 days under acidic conditions. The cell viability studies showed that both nanoparticles were safe toward mouse fibroblast cells (L929). Finally, both nanoparticles were found to be mucoadhesive in nature. Out of the two nanoparticulate systems developed, the gelatin lecithin nanoparticles demonstrates a strong potential as a carrier for donepezil delivery.
38.	Prominent Electrode Material for Na-, K-, and Mg-ion Batteries: 2D β-Sb Monolayer GA Shaikh, D Cornil, SK Gupta, R Ahuja, PN Gajjar – Energy & Fuels, 2022 **Abstract:** The applicability of a two-dimensional β-antimonene (β-Sb) monolayer as a negative electrode material for Na-, K-, and Mg-ion batteries has been conducted through first-principles calculations based on density functional theory (DFT). Our findings propose that the hollow and top sites are the energetically most stable adsorption sites for Na, Mg, and K atoms. The chronological adsorption energy, charge transfer, open-circuit voltage, theoretical storage capacity, and metal-ion diffusion barrier energy are investigated. The semiconducting β-Sb monolayer can provide inherent benefits for transportation of electrons through it, which can deliver tremendous mobility with lower barrier energies of 0.10 eV for Na, 0.09 eV for K, and 0.15 eV for Mg for the diffusion process. The double layers of β-Sb can adsorb ions on both sides, which leads, at high concentrations (Na_2Sb, K_2Sb, and Mg_2Sb), to theoretical storage capacities of 440.22, 440.22, and 880.45 mAh/gm for Na, K, and Mg ions, respectively. Besides, the electronic formation of β-Sb changed the nature from semiconducting to metallic under metal-ion adsorption, which significantly enhanced the performance of metal-ion batteries. With the given advantages, we propose that the β-Sb monolayer can be viewed as a potential material for negative electrodes in Na-, K-, and Mg-ion batteries.

	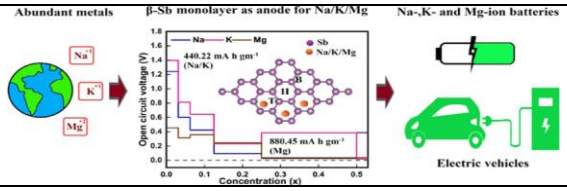
39.	Pure hydrogen and sulfur production from H_2S by an electrochemical approach using a NiCu-MoS_2 catalyst M Kumar, TC Nagaiah – Journal of Materials Chemistry A, 2022 **Abstract:** An enormous amount of hydrogen sulfide (H_2S) exists in an industrial world primarily as an undesirable waste by-product of fossil fuel processing, including natural gas, petroleum, and coal gasification, entailing a greener strategy for its conversion into more beneficial products viz. hydrogen (H_2) and sulfur (S). Herein, we have formulated a cost-effective and mixed-phase (1T and 2H) micro-flower like NiCu-MoS_2 catalyst towards the anodic sulfide oxidation reaction (SOR) and cathodic H_2 production via electrolysis. The SOR was initiated at 0.21 V vs. RHE, which is 1.02 V inferior to the thermodynamical potential of the oxygen evolution reaction (OER), i.e. 1.23 V. Moreover, it maintains 98.1% H_2 faradaic efficiency with remarkable endurance up to 150 h. Importantly when a H_2S electrolyzer was fabricated with NiCu-MoS_2, only 0.7 V cell potential was adequate to yield profuse H_2 by H_2S splitting, which is practically unachievable for water splitting due to kinetic and energetic complexity. 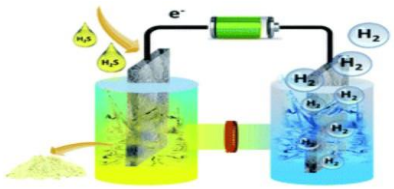
40.	Scheduling with Multiple Dispatch Rules: A Quantum Computing Approach PU Rao, B Sodhi – International Conference on Computational Science, 2022 **Abstract:** Updating the set of Multiple Dispatch Rules (MDRs) for scheduling of machines in a Flexible Manufacturing System (FMS) is computationally intensive. It becomes a major bottleneck when these rules have to be updated in real-time in response to changes in the manufacturing environment. Machine Learning (ML) based solutions for this problem are considered to be state-of-the-art. However, their accuracy and correctness depend on the availability of high-quality training data. To address the shortcomings of the ML-based approaches, we propose a novel Quadratic Unconstrained Binary Optimization (QUBO) formulation for the MDR scheduling problem. A novel aspect of our formulation is that it can be efficiently solved on a quantum annealer. We solve the proposed formulation on a production quantum annealer from D-Wave and compare the results with single dispatch rule based baseline model.
41.	Selective and sensitive determination of capsaicin using polymelamine formaldehyde decorated over carbon nanotubes D Mehta, N Thakur, TC Nagaiah – Materials Advances, 2022 **Abstract:** An electrochemical biosensor based on polymelamine formaldehyde (PMF) supported over oxygen functionalised carbon nanotubes (OCNTs) was designed for selective and sensitive determination of capsaicin. The synergy between the highly porous PMF and conductive OCNTs enhanced the electron transport at the electrode/electrolyte interface and eliminated the interference of common organic and inorganic ions at pH 1. The PMF/OCNT composite exhibited superior selectivity and sensitivity towards capsaicin with a low detection limit of 71.5 nM, a response time of ~1 minute and a wider detection range of 0.1-500 μM with two linear ranges of 100 nM-240 μM and 240-500 μM and high sensitivities of 960 μA μM^{-1} cm^{-2} and

	2900 μA μM^{-1} cm^{-2}, respectively. The proposed sensor was successfully applied to the determination of capsaicin in different chilli samples, with the recoveries between 99.2-114%, demonstrating the practical applicability of the sensor. 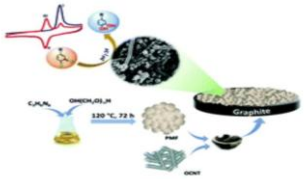
42.	Smartphone-based Surface Plasmon Resonance Sensors: a Review GP Singh, N Sardana – Plasmonics, 2022 **Abstract:** The surface plasmon resonance (SPR) is a phenomenon based on the combination of quantum mechanics and electromagnetism, which leads to the creation of charge oscillations on a metal–dielectric interface. The SPR phenomenon creates a signal which measures refractive index change at the metal–dielectric interface. SPR-based sensors are being developed for real-time and label-free detection of water pollutants, toxins, disease biomarkers, etc., which are highly sensitive and selective. Smartphones provide hardware and software capability which can be incorporated into SPR sensors, enabling the possibility of economical and accurate on-site portable sensing. The camera, screen, and LED flashlight of the smartphone can be employed as components of the sensor. The current article explores the recent advances in smartphone-based SPR sensors by studying their principle, components, application, and signal processing. Furthermore, the general theoretical and practical aspects of SPR sensors are discussed.
43.	Surface Nanopatterning of Amorphous Gallium Oxide Thin Film for Enhanced Solar-blind Photodetection D Kaur, P Vashishtha, G Gupta, S Sarkar, M Kumar – Nanotechnology, 2022 **Abstract:** Gallium oxide is an ultra-wide band gap semiconductor (E_g > 4.4 eV), best suited intrinsically for the fabrication of solar-blind photodetectors. Apart from its crystalline phases, amorphous Ga_2O_3 based solar-blind photodetector offer simple and facile growth without the hassle of lattice matching and high temperatures for growth and annealing. However, they often suffer from long response times which hinders any practical use. Herein, we report a simple and cost-effective method to enhance the device performance of amorphous gallium oxide thin film photodetector by nanopatterning the surface using a broad and low energy Ar^+ ion beam. The ripples formed on the surface of gallium oxide thin film lead to the formation of anisotropic conduction channels along with an increase in the surface defects. The defects introduced in the system act as recombination centers for the charge carriers bringing about a reduction in the decay time of the devices, even at zero-bias. The fall time of the rippled devices, therefore, reduces, making the devices faster by more than 15 times. This approach of surface modification of gallium oxide provides a one-step, low cost method to enhance the device performance of amorphous thin films which can help in the realization of next-generation optoelectronics.
44.	Unified modeling of unconventional modular and reconfigurable manipulation system A Dogra, S Mahna, SS Padhee, E Singla – Robotics and Computer-Integrated Manufacturing, 2022 **Abstract:** Customization of manipulator configurations using modularity and reconfigurability aspects is receiving much attention. Modules presented so far in literature deal with the conventional and standard configurations. This paper presents the 3D printable, light-weight and unconventional modules: MOIRs' Mark-2, to develop any custom n-Degrees-of-Freedom (DoF) serial manipulator even with the non-parallel and non-perpendicular jointed configuration. These unconventional designs of modular configurations seek an easy adaptable solution for both modular assembly and software interfaces for automatic modeling and control. A strategy of

	assembling the modules, automatic and unified modeling of the modular and reconfigurable manipulators with unconventional parameters is proposed in this paper using the proposed 4 modular units. A reconfigurable software architecture is presented for the automatic generation of kinematic and dynamic models and configuration files. Using these a designer can design and validate the models using visualization, plan and execute the motion of the developed configuration as required. The framework developed is based upon an open source platform called as Robot Operating System (ROS), which acts as a digital twin for the modular configurations. For the experimental demonstration, a 3D printed modular library is developed and an unconventional configuration is assembled, using the proposed modules followed by automatic modeling and control, for a single cell of the vertical farm setup.